D^* Mesons in photoproduction at HERA

H. Spiesberger[a]

[a]Institut für Physik, Johannes-Gutenberg-Universität Mainz,
Staudinger Weg 7, D-55099 Mainz, Germany

I describe the theoretical framework of the general-mass variable-flavor-number scheme for one-particle inclusive heavy-meson production and present numerical results for the photoproduction of D^* mesons at HERA.

1. Introduction

Progress in experimental techniques and increasing statistics at modern collider experiments are motivating us to work out predictions with improved precision for processes that involve heavy quarks. At HERA, the high precision of structure function measurements require a careful analysis of mass effects at higher orders of perturbative QCD for the contribution due to photon-charm scattering. Also the measurement of exclusive heavy-quark production has become an important tool to improve our understanding of strong interactions in general, as well as structure function data in particular. In the near future, at the LHC experiments, a detailed understanding of heavy-quark processes will be essential in many searches for new physics.

From the theoretical point of view, scattering processes with heavy quarks are particularly interesting, since the non-zero mass of the charm or bottom quark allows us to obtain reliable predictions from perturbative QCD also in situations where zero transverse momenta play a role, and the calculation of cross sections for massless quarks are obstructed by singular contributions.

The purpose of this article is to summarize the basic theoretical tools used in recent calculations of predictions for one-particle inclusive production of heavy mesons with charm or bottom quarks. In particular, I review the ideas underlying the *general-mass variable flavor-number scheme* (GM-VFNS), a framework that allows one to take into account not only effects due to non-zero quark masses, but also resummed logarithmic contributions which are important at high momenta. In particular, I will present results for the photoproduction of D^* mesons at HERA. Other contributions to the Ringberg workshop "New Trends in HERA Physics 2008" [1,2] have concentrated on aspects of heavy quarks for inclusive, i.e. structure function measurements.

2. Schemes for heavy quarks

Theoretical predictions for the production of heavy-quark mesons at high transverse momentum p_T are technically difficult to obtain due to the presence of the two different scales p_T and the heavy-quark mass m. On the one hand, the heavy-quark mass can be considered the large scale, since $m > \Lambda_{\rm QCD}$, making perturbative QCD applicable. When m is the only large scale, as for example in the calculation of the total cross section or in predictions of the p_T distribution close to the production threshold where p_T is of the same order of magnitude as m, predictions from a fixed-order calculation are reliable. On the other hand, if the transverse momentum p_T of the produced heavy quark is large compared with the heavy quark mass, $p_T \gg m$, then p_T should be used as the dominant large scale for the perturbative calculation and the quark mass can be neglected. In this case, large logarithms $\ln(p_T^2/\mu^2)$ arise at all orders, so that fixed-order perturbation theory is not valid anymore. These logarithms have to be resummed in order to obtain meaningful numerical predictions.

In the first case, for $p_T \lesssim m$, the traditionally used approach is called fixed flavor-number

scheme (FFNS) [3]. It is based on the assumption that the gluon and the light partons (u, d, s) are the only active partons. The heavy quark appears only in the final state, produced in the hard scattering process of light partons. The heavy-quark mass m is explicitly taken into account together with the transverse momentum p_T of the produced heavy meson assuming that m and p_T are of the same order. However, the complexity of such a calculation restricts one to the next-to-leading order, at present. In this scheme, the non-zero heavy-quark mass acts as a cutoff for initial and final-state collinear singularities. Instead of singular terms one finds logarithmic contributions containing $\log(p_T/m)$. Their presence restricts the applicability of the FFNS to the region of low transverse momenta; since $m \neq 0$ is retained in the calculation, predictions are reliable, on the other hand, close to the threshold of heavy-quark production.

In the second case, at large transverse momentum, the large logarithmic terms have to be resummed. In order to do that, one has to isolate these terms in the higher-order corrections to the hard scattering cross section and move them to parton distribution and fragmentation functions. The well-known factorization theorem provides the foundation of this re-ordering of higher-order corrections and there is a straightforward procedure for incorporating parton distribution and fragmentation functions into order-by-order perturbative calculations. Resummation of logarithmic contributions can then be obtained with the help of the DGLAP evolution equations. This approach requires therefore to treat the heavy quark as a parton, and as a consequence, one has to take into account additional processes where heavy quarks occur as incoming partons. Also, heavy mesons are not only produced by a non-perturbative transition from heavy quarks in the final state; in addition one has to consider processes where light partons fragment into the heavy meson. Since the heavy quark is treated like any other massless parton, quark or gluon, it is plausible to neglect the heavy-quark mass altogether. This approach is usually called zero-mass variable flavor-number scheme (ZM-VFNS). The parton distribution functions for heavy quarks and the fragmentation functions needed in this approach contain non-perturbative contributions and have to be obtained from a comparison with experimental data. Usually one assumes that these functions are zero below a starting scale, taken of the order of m. At this transition point, one switches from a description with n_f light partons to one with $n_f + 1$ partons. The predictions in this scheme are expected to be reliable only in the region of very large transverse momenta, since terms of the order of m^2/p_T^2 present in the hard-scattering cross sections are neglected.

In fact, it is not necessary to neglect the heavy-quark mass altogether in a variable flavor-number scheme. Instead, it is possible to absorb the large logarithms $\ln(p_T/m)$ into parton distribution and fragmentation functions where they are resummed by imposing DGLAP evolution, as in the ZM-VFNS, while at the same time, mass-dependent terms proportional to m^2/p_T^2 as obtained in the FFNS are retained in the hard-scattering cross section. This so-called general-mass variable-flavor number scheme (GM-VFNS) thus combines the virtues of the FFNS and the ZM-VFNS. The required subtraction of logarithmic terms, which are related to initial- and final-state singularities, can be defined with the usual $\overline{\rm MS}$ prescription. This guarantees the universality of parton distribution and fragmentation functions and allows for a meaningful comparison of data from different measurements.

It should be obvious that the partonic cross sections calculated in the FFNS are different from the corresponding ZM-VFNS cross sections, even in the limit $m \to 0$, since collinear singularities appear in different ways: in the first case, collinear emission of gluons from the heavy quark (see Fig. 1) leads to terms proportional to $\ln(p_T^2/m^2)$. In the zero-mass calculation of the ZM-VFNS, these singularities are obtained in the framework of dimensional regularization as poles in $1/\epsilon$ (where $\epsilon = D - 4$). The singularities are accompanied by different finite terms.

3. Mass Factorization and Subtractions

In order to determine the collinear singularities and their accompanying different finite terms, one

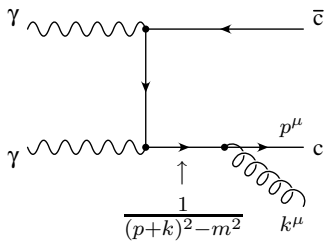

Figure 1. Gluon emission leads to the occurrence of collinear singularities: angular integration over the propagator $1/((p+k)^2-m^2) = 1/(2pk)$ gives rise to logarithms proportional to $\ln(p_T^2/m^2)$.

can proceed in two different ways. First, a direct comparison of a massless and a massive calculation is possible in a few cases where explicit NLO results are known in the two approaches. Then, the difference between the results from a calculation with non-zero mass in the limit $m \to 0$ and the results from a calculation with zero mass,

$$\Delta d\sigma = \lim_{m\to 0} d\tilde{\sigma}(m) - d\hat{\sigma}_{\overline{\rm MS}} \tag{1}$$

can be used to define subtraction terms,

$$d\sigma_{\rm sub} \equiv \Delta d\sigma \tag{2}$$

that allow one to obtain hard scattering cross sections including mass-dependent terms in the $\overline{\rm MS}$ factorization scheme:

$$d\hat{\sigma}(m) = d\tilde{\sigma}(m) - d\sigma_{\rm sub}\,. \tag{3}$$

Here, $d\hat{\sigma}_{\overline{\rm MS}}$ is the cross section obtained in a calculation where the heavy-quark mass is set to zero from the beginning and singularities are removed following the $\overline{\rm MS}$ prescription, while $d\tilde{\sigma}(m)$ denotes the cross section from a calculation with $m \neq 0$ where ultraviolet and collinear singularities due to massless partons have been removed also according to $\overline{\rm MS}$ factorization. The difference between the two calculations, i.e. the subtraction terms $d\sigma_{\rm sub}$ comprise logarithms of the heavy-quark mass as well as accompanying finite terms. The partonic cross section $d\hat{\sigma}(m)$ obtained after subtraction includes the complete regular m-dependence of the massive calculation, i.e. all terms proportional to powers of m^2/p_T^2 of $d\tilde{\sigma}(m)$.

After subtraction, the resulting partonic cross sections are defined in the conventional $\overline{\rm MS}$ factorization scheme in such a way that they can be combined with universal parton distribution functions $f_i^A(x,\mu_F)$ and fragmentation functions $d_k^H(z,\mu'_F)$, also defined in the $\overline{\rm MS}$ scheme, in the well-known factorization formula. Cross sections for hadronic processes, e.g. $A+B \to H+X$, can be obtained in the usual way:

$$\begin{aligned} d\sigma \;\; = \;\; & \sum_{i,j,k} f_i^A(x_1,\mu_F) \otimes f_j^B(x_2,\mu_F) \\ & \otimes d\hat{\sigma}(ij \to kX) \otimes d_k^H(z,\mu'_F)\,. \end{aligned} \tag{4}$$

As a consequence of factorization, at NLO, collinear logarithms of the type $\log(p_T^2/m^2)$ are separated into pieces $\log(p_T^2/\mu^2) + \log(\mu^2/m^2)$, introducing a factorization scale μ. In fact, these logarithms can be associated to either initial-state or final-state collinear emission of massless partons. Correspondingly, we can introduce two independent factorization scales for initial- and final-state singularities that we will denote by μ_F and μ'_F. In the first case, the terms containing $\log(\mu_F^2/m^2)$ are subtracted from the hard scattering cross section and absorbed in the parton distribution functions. In the second case, the logarithms $\log({\mu'_F}^2/m^2)$ are moved to the fragmentation functions. By imposing the DGLAP evolution equations on parton distribution and fragmentation functions, these logarithms can be resummed. Then, choosing μ_F and μ'_F of the order of p_T one can obtain predictions that are reliable also at large transverse momenta.

DGLAP evolution couples the set of parton distribution functions for light quarks and the gluon to those for the heavy quark. In a similar way, one needs fragmentation functions for the transition of not only the heavy quark to the considered heavy meson, but also fragmentation starting from light quarks and the gluon has to be taken into account and must be described by corresponding fragmentation functions. In any case one needs non-perturbative input, i.e. parton distribution and fragmentation functions must be fitted to experimental data. Usually one assumes

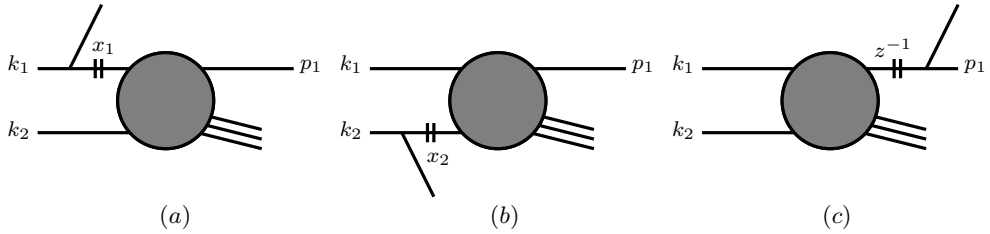

Figure 2. Sketch of kinematics of mass factorization in the case of one-particle inclusive particle production for (a) upper incoming line (b) lower incoming line and (c) outgoing line.

that there is a scale below which the parton distribution functions for heavy quarks vanish (no intrinsic charm or bottom). Also for fragmentation functions, initial conditions are prescribed for $c \to D$ (in the case of charm) at some initial scale and fragmentation from light quarks and gluons is assumed to vanish below the starting scale.

A second possibility for the calculation of subtraction terms is based on the fact that the mass singularities can be described by partonic parton distribution and fragmentation functions for collinear splittings $a \to b + X$. At next-to-leading order the required functions [4–6] are given for the initial state by

$$f^{(1)}_{g\to Q}(x,\mu_F^2) = \frac{\alpha_s(\mu_R)}{2\pi} P^{(0)}_{g\to q}(x) \ln\frac{\mu_F^2}{m^2}\,, \quad (5)$$

$$f^{(1)}_{Q\to Q}(x,\mu_F^2) = \frac{\alpha_s(\mu_R)}{2\pi} C_F \left[\frac{1+z^2}{1-z}(\ln\frac{\mu_F^2}{m^2} - 2\ln(1-z) - 1)\right]_+, \quad (6)$$

$$f^{(1)}_{g\to g}(x,\mu_F^2) = -\frac{\alpha_s(\mu_R)}{2\pi}\frac{1}{3}\ln\frac{\mu_F^2}{m^2}\delta(1-x)\,; \quad (7)$$

and for final-state splittings by

$$d^{(1)}_{g\to Q}(z,{\mu'_F}^2) = \frac{\alpha_s(\mu_R)}{2\pi} P^{(0)}_{g\to q}(z) \ln\frac{{\mu'_F}^2}{m^2}\,, \quad (8)$$

$$d^{(1)}_{Q\to Q}(z,{\mu'_F}^2) = C_F\frac{\alpha_s(\mu_R)}{2\pi} \left[\frac{1+z^2}{1-z}(\ln\frac{{\mu'_F}^2}{m^2} - 2\ln(1-z) - 1)\right]_+. \quad (9)$$

Other partonic distribution and fragmentation functions are zero to this order in α_s. They can be viewed as describing the transition from a massless to a massive parton and vice versa in the limit where the mass can be neglected in comparison with the typical energy or momentum of the hard scattering process. The complete logarithmic dependence on the heavy-quark mass can be factorized into these functions and the partonic higher-order subprocess cross section is obtained by convolutions of these functions with subtracted partonic cross sections that are well-behaved and finite in the limit $m \to 0$. Figure 2 shows a sketch of this factorization. The subtraction terms needed in the GM-VFNS can therefore also be obtained as convolutions, at NLO as convolutions of the partonic distribution and fragmentation functions given above, with the subprocess cross sections at LO.

For example, the direct contribution to heavy-quark photoproduction contains a term coming from the subprocess $\gamma^* + g \to Q + \bar{Q} + g$. The logarithmic m-dependence due to the splitting $g \to Q + \bar{Q}$ in the initial state can be factorized into the partonic distribution function $f_{g\to Q}(x,\mu^2)$. The subtraction term related to this contribution is thus obtained as (see Fig. 2a)

$$d\sigma_{\rm sub}(\gamma^* g \to QX) = \int_0^1 dx_1\; f^{(1)}_{g\to Q}(x_1,\mu_F^2) \times d\hat{\sigma}^{(0)}(\gamma^* Q \to QX)[x_1 k_1, k_2, p_1] \equiv f^{(1)}_{g\to Q}(x_1) \otimes d\hat{\sigma}^{(0)}(\gamma^* Q \to QX)\,. \quad (10)$$

Other terms contain mass logarithms that lead to subtractions in the final state where the partonic fragmentation function $d_{Q\to Q}(z,\mu^2)$ is needed.

For resolved contributions one has to take into account additional subtraction terms that involve partonic distribution functions for incoming quarks or gluons from the resolved photon, for example (see Fig. 2b),

$$d\sigma_{\rm sub}(ab\to QX) = \int_0^1 dx_2\; f^{(1)}_{b\to j}(x_2,\mu_F^2) \qquad (11)$$
$$\times d\hat{\sigma}^{(0)}(aj\to QX)[k_1,x_2k_2,p_1]$$
$$\equiv f^{(1)}_{b\to j}(x_2)\otimes d\hat{\sigma}^{(0)}(aj\to QX)\,,$$

where in principle any combination of partons a and b contribute, but only few combinations are non-zero at next-to-leading order (see Eqs. (5-7)). Similarly, subtraction terms involving the partonic fragmentation functions $d_{Q\to Q}(z,\mu^2)$ and $d_{g\to Q}(z,\mu^2)$ to absorb mass logarithms arising from singular $g\to Q$ or $Q\to Q$ splittings are needed (see Fig. 2c),

$$d\sigma_{\rm sub}(ab\to QX) =$$
$$\int_0^1 dz d\hat{\sigma}^{(0)}(ab\to kX)[k_1,k_2,z^{-1}p_1]d^{(1)}_{k\to Q}(z,{\mu'_F}^2)$$
$$\equiv d\hat{\sigma}^{(0)}(ab\to kX)\otimes d^{(1)}_{k\to Q}(z)\,.$$

The partonic distribution and fragmentation functions are explicitly known and the subtraction terms can therefore be calculated analytically at next-to-leading order [7]. The results have been compared to the expressions that we found from a comparison of massive and massless calculations as described above. Differences that we found in an early stage of our work could be attributed in the meantime to errors in the published results for the next-to-leading order corrections in the massive calculation [8] so that our calculations are now based on a reliable set of formulas.

4. Photoproduction of D^* Mesons

The particular complication in a calculation of predictions for photoproduction processes is due to the fact that two interaction modes contribute: first, the photon can scatter off a parton originating from the proton through a point-like coupling (direct contribution) and, secondly, the photon can act as a source of partons which scatter off the partons from the proton through the strong interaction (resolved contribution). At leading order, the two interaction mechanisms appear to be independent, but at next-to-leading order, the separation into direct and resolved contributions is scheme dependent since singular corrections to the direct part have to be factorized into parton distribution functions of the photon. It is therefore important that direct and resolved parts are treated in a consistent way.

Our first results for the photoproduction process $\gamma + p \to D^* + X$ [9] were based on results obtained earlier in a study of the process $\gamma+\gamma\to D^*+X$ [10,11]. Those early calculations were sufficient to set up the GM-VFNS framework for the direct contribution. In Ref. [9], the resolved contribution was still evaluated in the ZM-VFNS. Now, results for $p+\bar{p}\to D^*+X$ [12,7] are available and we have used them to extend the GM-VFNS prescription also to the resolved process. In the following I describe numerical results for photoproduction of D^* mesons based on a complete NLO calculation where all parts are consistently obtained in the GM-VFNS.

A second improvement of our earlier results [9] concerns the incorporation of improved fragmentation functions for D^* mesons. These new fragmentation functions have been obtained in Ref. [13] and are based on a comparison of recent experimental data for $e^+ + e^- \to D^* + X$ of the CLEO [14] and Belle [15] collaborations with theoretical predictions that are also based on the GM-VFNS. For the first time it is therefore possible to analyze experimental data in a fully consistent framework based on the GM-VFNS.

4.1. Numerical Results

Measurements of inclusive $D^{*\pm}$ meson production in photon-proton collisions have been performed by the two collaborations H1 and ZEUS since the beginning of HERA experiments. The most recent results have been made public in Refs. [16,17] (for previous measurements, see [18,19]). Photoproduction in ep collisions at HERA is characterized by an almost vanishing virtuality ($Q^2\simeq 0$) of the exchanged photon. Ex-

perimentally, low Q^2 events are isolated in different ways in the two experiments and the photoproduction cross section defined by either imposing a cut on Q^2 or on the electron scattering angle. For the numerical results to be discussed below, we decided to use the kinematic region relevant for a comparison with the most recent H1 data. Our previous comparison with ZEUS data [9] can be updated as soon as their more recent measurements will have been finalized.

Kinematical cuts have been implemented as follows: the energies of the incoming protons and electrons (positrons) are $E_p = 920$ GeV and $E_e = 27.5$ GeV. The total center-of-mass energy W of the γp process is restricted to the range $100 < W < 285$ GeV, corresponding to cuts on the inelasticity y_e of $0.1 < y_e < 0.8$. The maximal value of Q^2 used as anti-tagging condition in the experimental analysis is $Q^2 < 2$ GeV^2. The rapidity is defined in the reference frame of the HERA experiments with positive η in the direction of the incoming proton. In the following, the transverse momentum distribution is calculated with a cut in the rapidity η of the D^* meson, $|\eta| \leq 1.5$, and presented as a histogram using nine bins of varying widths as in the H1 experiment starting at $p_T = 1.8$ GeV and extending up to 12.5 GeV. When we give results for the rapidity distribution we will integrate over the transverse momentum in the range $1.8 \leq p_T \leq 12.5$ GeV, again as in the experimental results.

As input for the parton distribution functions we have used the CTEQ6.5 parametrization for the proton PDFs [20] and the set GRV92 for the photon PDFs [21]. The latter ones have been transformed to the $\overline{\rm MS}$ scheme. The set CTEQ6.5 for the proton PDFs is the result of a first global analysis of the CTEQ group with heavy quark mass effects in the ACOTχ prescription taken into account. The fragmentation u, d, s, c, $g \to D^*$ is described by the purely non-perturbative Global-GM fit described in Ref. [13]. We choose for the renormalization scale μ_R and the factorization scales μ_F and μ'_F corresponding to the subtraction of initial and final state singularities equal values and set $\mu_R = \xi_R m_T = \xi_R\sqrt{m^2+p_T^2}$, $\mu_F = \xi_F m_T$ and $\mu'_F = \xi'_F m_T$ with $\xi_R = \xi_F = \xi'_F = 1$. α_s is calculated from the two-loop formula [22] with $n_f = 4$ and $\Lambda^{(n_f=4)}_{\overline{\rm MS}} = 328$ MeV corresponding to $\alpha_s(m_Z) = 0.118$. The charm mass is taken to be $m = 1.5$ GeV.

Mass terms proportional to powers of m^2/p_T^2 enter in subprocesses where the heavy quark is created through scattering of light particles. In the direct contribution, these are the process $\gamma + g \to c + \bar{c}$ at leading order, where the gluon originates from the proton; virtual corrections to this process combined with the gluon bremsstrahlung process $\gamma + g \to c + \bar{c} + g$; and the next-to-leading order subprocess $\gamma + q(\bar{q}) \to c + \bar{c} + q(\bar{q})$, where q denotes a light quark. Explicit expressions for these cross sections and the subtraction terms needed for the transition to the GM-VFNS with $\overline{\rm MS}$ renormalization and factorization can be found for the abelean part in [10] and for the non-abelean part in [11]. For the resolved contribution one has to consider the processes $g + g \to c + \bar{c}$ and $q + \bar{q} \to c + \bar{c}$ at leading order; virtual and bremsstrahlung corrections to the leading-order processes; and the next-to-leading subprocess $g + q(\bar{q}) \to c + \bar{c} + q(\bar{q})$. In addition, the direct and resolved parts contain contributions from scattering processes where one or both of the incoming partons are replaced by a charm or an anti-charm quark. These latter processes have to be calculated with $m = 0$ since here the heavy quark is treated as a parton. Finally, also subprocesses where both incoming and outgoing partons are light quarks or gluons contribute through fragmentation of light quarks and gluons to the heavy meson.

Mass terms are expected to be sizable at low p_T, but should vanish with increasing p_T. In Fig. 3 we display the ratio of predictions for the differential cross section $d\sigma/dp_T$ obtained from the calculation with $m \neq 0$ in the GM-VFNS and the zero-mass calculation in the ZM-VFNS. For the direct contribution, the ratio $d\sigma(m \neq 0)/d\sigma(m = 0)$ reaches the value of 0.7 in the first p_T-bin with $p_T \simeq 2$ GeV, but increases rapidly with increasing p_T and reaches 0.96 in the highest p_T-bin with $p_T \simeq 12$ GeV. The reduction of the direct cross section due to finite mass effects is thus significant for $p_T \lesssim 3.5$ GeV. In Fig. 3 we also show the ratio of cross sections in the massive and

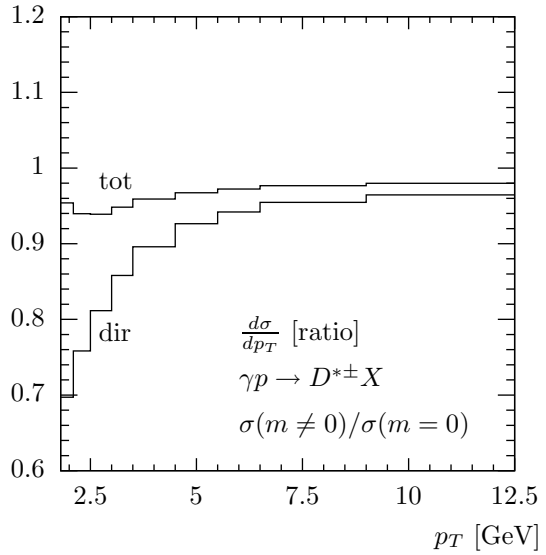

Figure 3. The effect of mass-dependent terms on the direct contribution (lower line) and the total cross section (upper line) for $\gamma + p \to D^* + X$.

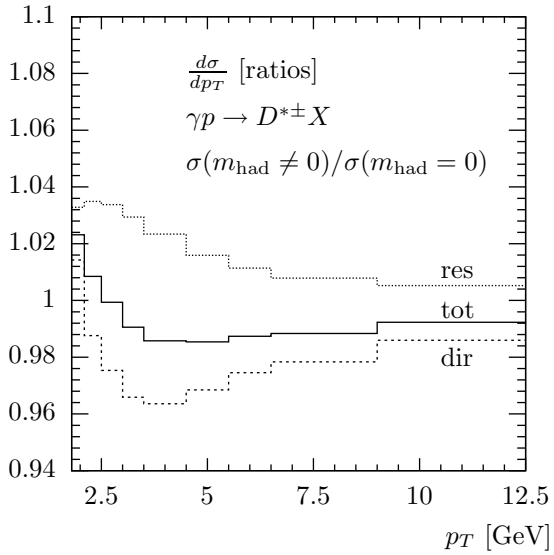

Figure 4. The influence of the D^* meson mass on the direct contribution (lower dashed line), the resolved contribution (upper dotted line) and the total cross section (full line) for $\gamma + p \to D^* + X$ (see text).

the massless calculation for the sum of the direct and the resolved part, denoted "tot" in the figure. This ratio is almost constant as a function of p_T and varies between 0.94 and 0.98 in the considered range of p_T values. Mass corrections turn out to be smaller for the total cross section for two reasons: first, terms containing powers of m^2/p_T^2 enter with different signs in the direct and the resolved contributions and cancel in the sum: secondly, the total cross section contains contributions with a charm quark in the initial state which are evaluated with zero mass since the heavy quark is treated as a parton in this case, i.e. only part of the complete cross section carries a mass dependence. The same ratio as a function of η shows more prominent mass effects and the shape of the η-distribution is more strongly affected. At negative rapidities, the sum of direct and resolved parts is decreased by charm mass effects by up to 16 % in the first bin, while for positive rapidities the cross section is increased by about +50 % in the bin with largest η values.

Mass-dependent terms introduce an additional sensitivity on the value of the charm-quark mass. Varying m by ± 0.3 GeV around its default value of 1.5 GeV, we observe a change of the p_T distribution by a few per cent: the uncertainties are largest at small p_T of roughly ± 6 %, but decrease to values below 1 % at large p_T. The dependence on m does not add further to the change of the shape of the η distribution; here the differential cross section is affected by ± 6 % uncertainties at negative η and the uncertainty is again decreasing towards positive η.

In the calculation described above, we have identified the rapidity of the inclusively produced c quark with the pseudo-rapidity of the D^* meson and only the transverse momentum is scaled down when folding with the fragmentation function $D(z)$. This corresponds to neglecting the mass of the D^* meson. In fact, there is an inherent ambiguity in the definition of the scaling variable z and the way how to take into account the hadron mass. To estimate the corresponding uncertainties of our predictions, we have studied the alternative to define the scaling variable by the ratio of the +-components of the quark and meson momenta, $p^+_{D^*} = z p^+_c$ where $p^+ = E + p_L$ and p_L is the longitudinal momentum in the γp center of mass system. Taking into account the

D^* meson mass ($m_{D^*} = 2.01$ GeV) one obtains numerical results for the p_T distribution as shown in Fig. 4. The curves represent the ratios of the cross sections with $m_{\rm had} \neq 0$ and scaling the +-components of the momenta over those with $m_{\rm had} = 0$. The ratios are also calculated separately for the direct contribution (dashed curve) and the resolved contribution including the parts with charm quarks in the initial state (dotted curve). For the total cross section $d\sigma/dp_T$, the ratio is close to one; except for the first two p_T-bins where we see an enhancement of up to 2 %, we find a small suppression by not more than 1.2 %. However, the shape of the η-distribution, $d\sigma/d\eta$ is again more strongly affected. At negative rapidities we find a suppression reaching 14 % in the first η-bin and at positive rapidities the cross section is enhanced by up to 10 % in the last η-bin. Since there is no strong theoretical justification to prefer one over the other prescription to take into account these kinematic mass effects, we have neglected this effect in the comparison with HERA data that I describe in the following.

4.2. Comparison with HERA Data

For a comparison with preliminary experimental data from the H1 collaboration [17] we have calculated differential cross sections with kinematical cuts as defined in the experimental analysis. A meaningful interpretation requires knowledge of the uncertainties of the theoretical predictions. A detailed study [23] has shown that the dominating source of uncertainties is due to the ambiguity in the choice of the renormalization and factorization scales. Uncertainties due to the value of the charm mass and the choice of parton distribution and fragmentation functions are much smaller. In the following we therefore compare with predictions where the scales are taken proportional to the transverse mass $m_T = \sqrt{p_T^2 + m^2}$ with coefficients that are varied between 1/2 and 2, i.e. we fix $\mu_i = \xi_i m_T$ for $i = R$, F and F' and for ξ_i we choose values $\xi_i = \frac{1}{2}$, 1, 2 in such a way that $\xi_F = \xi'_F$ and $1/2 \leq \xi_F/\xi_R \leq 2$. We determine the maximal and minimal cross section from calculations with the five different choices $(\xi_R, \xi_F, \xi'_F) = (\frac{1}{2}, 1, 1)$, $(1, 2, 2)$, $(1, 1, 1)$, $(2, 1, 1)$ and $(1, \frac{1}{2}, \frac{1}{2})$ and display in the following the resulting error band.

The maximal cross section is found for $\xi_R = \frac{1}{2}$, $\xi_F = \xi'_F = 1$, the minimal one for $\xi_R = 2$, $\xi_F = \xi'_F = 1$ if $p_T \gtrsim 3$ GeV and $\xi_R = 1$,

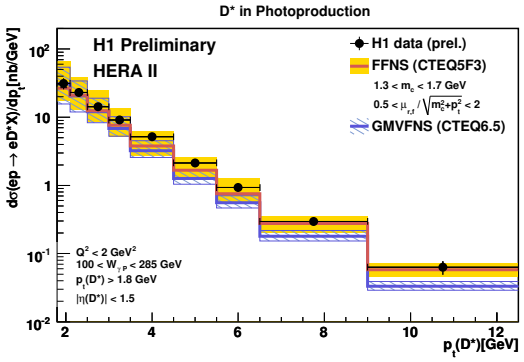

Figure 5. Comparison of NLO predictions in the GM-VFNS for $d\sigma/dp_T$ (hashed (blue) band) with H1 preliminary data [17] for $\gamma + p \to D^* + X$. The shaded (yellow) band shows the prediction of a calculation in the fixed-flavor number scheme [3] (see text for further details, colors in the electronic version).

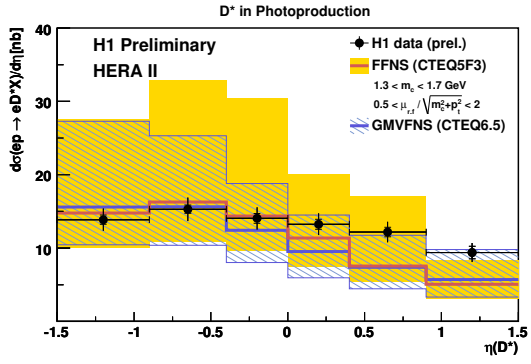

Figure 6. As Fig. 5 for the rapidity distribution $d\sigma/d\eta$.

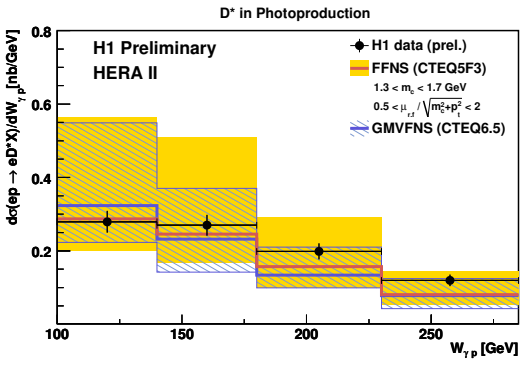

Figure 7. As Fig. 5 for the distribution with respect to the total γp center-of-mass energy, $d\sigma/dW_{\gamma p}$.

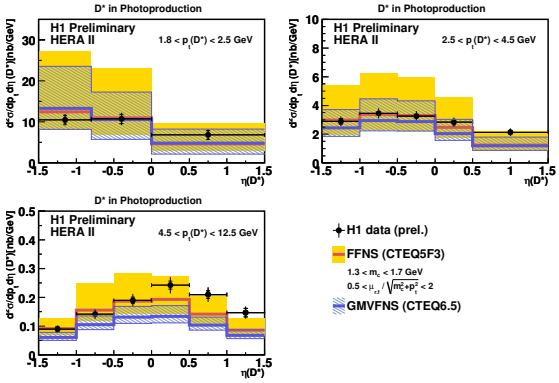

Figure 8. The double-differential distributions $d^2\sigma/dp_T d\eta$ for three bins of p_T: preliminary H1 data [17] are compared with GM-VFNS and FFNS predictions, as in Fig. 5.

$\xi_F = \xi'_F = \frac{1}{2}$ for $p_T \lesssim 3$ GeV. Apart from the region of low p_T values, the maximal (minimal) cross section as a function of p_T is controlled by the renormalization scale factor $\xi_R = \frac{1}{2}\,(2)$. Only for small p_T values the minimal cross section is obtained for the smallest $\xi_F = \xi'_F = \frac{1}{2}$. The scale variation of the cross section is largest for the smallest p_T bin as expected. $d\sigma/dp_T$ is changed by $+84\,/-53\%$ compared to the result with the default choice $\xi_R = \xi_F = \xi'_F = 1$. In the largest p_T bin the corresponding change is only $+13\,/-16\%$. For the η-distribution the scale variation is large over the whole considered range and dominated by the contribution from small values of p_T, due to the small cut $p_T \geq 1.8$ GeV. In the most negative (positive) η-bins the scale change is $+76\,/-36\,\%$ $(+74\,/-46\,\%)$ compared to the default cross section.

In Figs. 5 – 8 we show the comparison of our predictions with preliminary data from H1. In general, the data points fall inside the error band of theoretical predictions, except for the largest p_T where the data are above the GM-VFNS calculation, discrepancies being largest for positive rapidities. The figures contain also predictions that were obtained from a calculation in the fixed-flavor number scheme [3].

In summary, I have presented numerical results for the photoproduction of D^* mesons, obtained at next-to-leading order in the general-mass variable flavor-number scheme. This approach combines the virtues of a zero-mass calculation where large logarithmic corrections are resummed in universal parton distribution and fragmentation functions, and those of a finite-mass calculation where finite mass terms are kept. The results presented here are based on an improved study where the GM-VFNS approach is used also for the calculation of the resolved contributions. In addition, new parametrizations for D^* fragmentation functions have been used to obtain numerical predictions for p_T and rapidity distributions that can be compared to experimental data from HERA.

Effects from finite mass-dependent contributions are found to be important at small p_T and for the shape of the η distribution, first of all for the direct part. However, the presence of charm-initiated contributions, which are calculated with zero mass, and cancellations between mass-dependent terms in the direct and the resolved contribution, lead to a suppression of mass effects in the complete cross section. Uncertainties due to the value of the charm mass, the parton distribution functions in the proton and in the

photon, and fragmentation functions are found to be roughly in the order of 10 %, whereas variations of the renormalization and factorization scales lead to appreciable uncertainties.

Acknowledgment

I thank B. A. Kniehl, G. Kramer and I. Schienbein for a fruitful collaboration from which the results presented in this article have emerged. I also acknowledge discussions with K. Lipka and K. Urban on the experimental data.

REFERENCES

1. F. Olness, this volume.
2. R. Thorne, this volume.
3. S. Frixione, M. Mangano, P. Nason and G. Ridolfi, Phys. Lett. B **348** (1995) 633; S. Frixione, P. Nason and G. Ridolfi, Nucl. Phys. B **545** (1995) 3, and earlier references given therein.
4. B. Mele and P. Nason, Nucl. Phys. B **361** (1991) 626.
5. S. Kretzer and I. Schienbein, Phys. Rev. D **58** (1998) 094035; Phys. Rev. D **59** (1999) 054004.
6. K. Melnikov and A. Mitov, Phys. Rev. D **70** (2004) 034027; A. Mitov, Phys. Rev. D **71** (2005) 054021.
7. B. A. Kniehl, G. Kramer, I. Schienbein and H. Spiesberger, Eur. Phys. J. C **41** (2005) 199.
8. Z. Merebashvili, A. P. Contogouris and G. Grispos, Phys. Rev. D **62** (2000) 114509; Erratum-ibid. D **69** (2004) 019901.
9. G. Kramer and H. Spiesberger, Eur. Phys. J. C **38** (2004) 309.
10. G. Kramer and H. Spiesberger, Eur. Phys. J. C **22** (2001) 289.
11. G. Kramer and H. Spiesberger, Eur. Phys. J. C **28** (2003) 495.
12. B. A. Kniehl, G. Kramer, I. Schienbein and H. Spiesberger, Phys. Rev. D **71** (2005) 014018.
13. T. Kneesch, B. A. Kniehl, G. Kramer and I. Schienbein, Nucl. Phys. B **799** (2008) 34.
14. M. Artuso *et al.* [CLEO Collaboration], Phys. Rev. D **70** (2004) 112001.
15. R. Seuster *et al.* [Belle Collaboration], Phys. Rev. D **73** (2006) 032002.
16. ZEUS Collaboration, *Measurement of D^* photoproduction at HERA* (2003), `http://www-zeus.desy.de/public_plots`; see also S. Chekanov, 31st International Conference on High Energy Physics, ICHEP 02, July 24-31, 2002, Amsterdam, Abstract 786.
17. H1 Collaboration, H1prelim-08-073, *Measurement of the D^* production cross section in photoproduction with the H1 detector using HERA II data*, `http://www-h1.desy.de/h1/www/publications`; A. Jung [H1 Collaboration], Proc. XVI Int. Workshop on Deep Inelastic Scattering, DIS 2008, April 7-11, 2008, London, `http://dx.doi.org/10.3360/dis.2008.196`.
18. J. Breitweg *et al.* [ZEUS Collaboration], Eur. Phys. J. C **6** (1999) 67, and earlier references given therein.
19. A. Aktas *et al.* [H1 Collaboration], Eur. Phys. J. C **50** (2007) 251, and earlier references given therein.
20. W.-K. Tung *et al.* [CTEQ Collaboration], JHEP **0702** (2007) 053.
21. M. Glück, E. Reya and A. Vogt, Phys. Rev. D **46** (1992) 1973.
22. W.M. Yao *et al.* [Particle Data Group], J. Phys. G **33** (2006) 1.
23. B. A. Kniehl, G. Kramer, I. Schienbein and H. Spiesberger, preprint DESY 08-204, arXiv:0902.3166 [hep-ph].